NIH Public Access
Author Manuscript
Wound Repair Regen. Author manuscript; available in PMC 2011 March 1.

Published in final edited form as:
Wound Repair Regen. 2010 ; 18(2): 235–244.

Occlusion Regulates Epidermal Cytokine Production and Inhibits Scar Formation

Corrie L Gallant-Behm, PhD and **Thomas A Mustoe, MD**
Division of Plastic and Reconstructive Surgery, Northwestern University, Chicago, IL, USA

Abstract

Hypertrophic scars are a major clinical problem, yet there are few therapeutics available to prevent or treat scar formation. One of the oldest known and most effective treatments is occlusion with silicone gel. However, little is known about its mode of action. It is hypothesized that occlusion increases the hydration state of the epidermis, and that this affects the epidermal and dermal cell behavior. This study investigated that possibility. Using the rabbit hypertrophic scar model, we determined that occlusion was able to increase the hydration state of the epidermis in a dose dependent manner, and significantly reduced the scar hypertrophy. Quantitative RT-PCR and immunohistochemistry demonstrated that occlusion altered the keratinocyte behavior, including keratin expression. Furthermore, occlusion significantly decreased the epidermal expression of the pro-fibrotic cytokine IL-1β and increased the epidermal expression of the anti-fibrotic cytokine TNF-α. Those alterations in epidermal gene expression resulted in concomitant changes in the expression of TGF-β family members by cells in the dermis, resulting in a decrease in pro-fibrotic signaling within the dermis. In summary, the results of this study indicate that occlusive therapy was able to decrease dermal fibrosis by hydrating the epidermis and altering the pro- and anti-fibrotic signals produced following injury.

Keywords

Hypertrophic scarring; wound repair; fibrosis; occlusion; epidermis

Introduction

Cutaneous wounds frequently heal with the formation of a clinically significant scar, such as hypertrophic scars or keloids. Such scars are a major concern, as they can be painful or pruritic, are less elastic and less strong than unwounded skin, and may profoundly affect a patient's psychosocial state. One of the few accepted clinical modalities for reducing the incidence of hypertrophic scarring in susceptible individuals is the occlusion of an injury site with silicone gel sheeting (1–3) or with topical silicone gel (4) (review). Silicone gel has also been shown to be effective in the rabbit ear model of hypertrophic scarring (5,6), and supplementation of this treatment with additional occlusive dressings has been shown to increase its efficacy (7). Furthermore, non-silicone based occlusion methods alone have been shown to reduce epidermal hyperproliferation (as measured by thickness, cellularity, and mitotic activity) in a rat incision model (8) as well as in the rabbit hypertrophic scar model (6). These findings suggest that the mechanism of action of silicone gel sheeting is its ability to occlude the skin (4,9), and not due to the chemistry of the material or due to its oxygen permeability (7). This hypothesis is supported by the observation that silicone oil

Corresponding author & reprint requests: Thomas A. Mustoe, 675 N. St Clair St, 19th Floor Galter, Suite 215, Chicago, IL 60611 USA, tmustoe@nmh.org, Phone: 1-312-695-6022.

NIH-PA Author Manuscript
NIH-PA Author Manuscript
NIH-PA Author Manuscript

NIH-PA Author Manuscript

NIH-PA Author Manuscript

NIH-PA Author Manuscript

alone, which is not occlusive, is not an effective therapeutic, but silicone oil when combined with an occlusive dressing is effective at reducing the thickness and improve the appearance of pre-existing hypertrophic scars and keloids without surgical intervention (10). Nonetheless, the mechanism of action of occlusive therapy is poorly understood.

There is an increasing body of evidence that suggests that keratinocytes may influence fibroblast behavior, and that this cellular interaction is affected by the hydration state of the keratinocytes. Investigations in this laboratory (11) and others (12) have determined that fibroblasts reduce their rate of collagen synthesis when co-cultured with keratinocytes *in vitro* (11,12). Furthermore, this effect was enhanced when the keratinocytes were hydrated, but not when non-occlusive materials such as silicone oil or paraffin were added to the keratinocytes (12). Additional investigations have determined that hydrated keratinocytes secrete less interleukin-1 beta (IL-1β) and more tumor necrosis factor-alpha (TNF-α) than do air-exposed keratinocytes (11).

Taken together, the clinical, *in vivo*, and *in vitro* data support the hypothesis that keratinocytes regulate fibroblast behavior through the production of pro- and anti-fibrotic soluble factors, and that the production of those factors is dependent on the hydration state of the keratinocytes. The current study was designed to investigate this hypothesis using an established animal model of hypertrophic scarring, the New Zealand White rabbit ear punch model. We investigated the hydration state of the epidermis, the degree of keratinocyte differentiation, and the expression of pro- and anti-fibrotic signals by the epidermis following varying amounts of occlusive therapy. We have also correlated those effects with the expression of pro-fibrotic growth factors and signaling molecules in the dermis. These studies provide new information on the role of silicone gel and other occlusive therapeutics in regulating scar formation, and on how the epidermis may regulate dermal extracellular matrix synthesis *in vivo*.

Materials and Methods

Hypertrophic scar model

A reproducible model of hypertrophic scar formation in the New Zealand White rabbit was utilized as previously described (13), with minor modifications outlined below. All animal investigations were performed in compliance with institutional guidelines and under the National Research Council's criteria for humane care as outlined in the "Guide for the Care and Use of Laboratory Animals". Briefly, female animals (3.5–5kg, N=3) were anesthetized with ketamine (45mg/kg) and xylasine (7mg/kg). Following depilation and a surgical scrub, local anesthetic (1% lidocaine HCl and 1:100,000 epinephrine) was injected subcutaneously at six sites on the ventral surface of each ear. At each site, a 7mm diameter biopsy punch was used to score the skin to the depth of the cartilage, and the epidermis and dermis was removed, leaving the perichondrium intact. All wounds were dressed with one layer of adhesive Tegaderm dressing (3M, St Paul, MN), and the animals were given post-operative analgesia (buprenorphine 0.05mg/kg) every 8–12 hours for 24 hours post-surgery. The wounds were monitored daily for infection, and the dressings were replaced as necessary until complete re-epithelialization was observed on post-operative day 18 (POD18).

Scar treatments

Following complete re-epithelialization (POD 18), all dressings were removed. The wounds were randomized into treatment groups and graded levels of occlusion were applied to the scars (N=9 wounds per treatment). One group of control wounds remained un-occluded. The second group of wounds had a single layer of adhesive semi-occlusive Tegaderm dressing applied so as to cover all of the wounds. A third group had five layers of Tegaderm applied

NIH-PA Author Manuscript

NIH-PA Author Manuscript

NIH-PA Author Manuscript

on top of one another, and applied to the ear to cover the wounds. The Tegaderm dressings were changed every two days from POD18 until POD28, at which time maximal scar hypertrophy is typically observed (13).

In vitro validation of graded occlusion

The model of graded occlusion was validated *in vitro* by measuring the water vapor loss from a water-saturated sponge (35mm × 25mm × 2mm biopsy foam pad, Fisher Scientific, Houston, TX) covered with increasing numbers of layers of Tegaderm semi-occlusive dressing (1 layer to 6 layers, applied on top of one another, 5cm × 5cm in size). One sheet of silicone gel sheeting (Cica-Care, Smith & Nephew) held down by one layer of Tegaderm was used as the standard-of-care control. Water vapor loss through the dressings was measured using a TEWAMETER TM210 (Courage + Khazaka Electronic GmbH). All measurements were performed under standardized environmental conditions (21°C, 35% humidity). Specifically, the TEWAMETER probe was applied to the relevant surface for a period of no less than 1.5 minutes and no more than 7 minutes. When the measurement for moisture loss (reported in g/m^2/hour) achieved stability (standard deviation <0.1 g/m^2/hour), the values were recorded. All measurements were repeated five times.

In vivo skin hydration and trans-epidermal water loss (TEWL) measurements

At day 28 post-wounding, the Tegaderm dressings were removed and all wounds were blotted dry. The skin hydration at each wound site was measured using a Skicon-200 skin surface hygrometer (I.B.S. Co., Hamamatsu, Japan). This instrument measures the conductance of the skin, and values are reported in μ·s. Specifically, the animals were subjected to gentle restraint, and the Skicon-200 probe was applied to the center of each wound site for a total of three seconds. Each measurement was repeated five times and the mean of the five readings was used. The wounds were then allowed to acclimatize to room air for 2 hours, to allow any additional surface water to evaporate. The animals were then anaesthetized as described for the initial surgeries, and the trans-epidermal water loss (TEWL) of each wound was measured using the TEWAMETER TM210 (Courage + Khazaka Electronic GmbH) as described above.

Tissue harvest and preparation

Following the completion of the skin hydration and TEWL measurements, the anesthetized animals were euthanized via an overdose of intracardiac Euthasol (pentobarbital sodium and phenytoin sodium). All wounds were photographed and harvested using a 10 mm biopsy punch. Half of each wound was snap frozen in liquid nitrogen for molecular analysis and half was fixed overnight in 10% zinc formalin for histological analysis. Samples from normal, unwounded skin were harvested and processed in the same manner.

Histology

All samples were embedded in paraffin (Paraplast X-tra, Fisher Scientific, Houston, TX) and were sectioned at 5μm thickness through the center of each wound. Serial sections were deparaffinized and stained with either hematoxylin and eosin (14), Sirius red in picric acid (15), safranin O and fast green (16), or alcian blue (pH 2.5) (17). The hematoxylin and eosin stained sections were photographed under 10x and 20x magnification and were used for quantifying the total scar area (scar elevation index, SEI) (13) using ImageJ software (NIH, Bethessa, MD). A SEI value of 1 indicates that the scar dermis is of an equivalent height to the dermis of the adjacent normal, unwounded skin. A SEI value of 2 indicates that the height of the scar dermis is twice that of unwounded skin. The Sirius red stained sections were photographed under cross-polarized light microscopy at 20x magnification and were used for evaluating the density of dermal collagen fibers (15). Mature collagen fibers stain

NIH-PA Author Manuscript

NIH-PA Author Manuscript

NIH-PA Author Manuscript

orange/red, and immature collagen fibers stain yellow/green. The safranin O/fast green and alcian blue stained sections were photographed under 20x magnification and were used to evaluate the density of dermal proteoglycan deposits. Safranin O stains proteoglycans red and alcian blue stains proteoglycans blue. In all cases, qualitative analysis was performed by 3–8 blinded observers experienced in performing histologic analysis of human and rabbit skin wounds and hypertrophic scars. In addition, quantitative analysis of the Sirius red staining intensity was performed using ImageJ.

Immunohistochemistry

Immunohistochemistry for keratin 5 and keratin 10 was performed. Five-micron thick paraffin sections were deparaffinized, rehydrated, and antigen retrieval was performed in 1x citrate buffer (Lab Vision Corp, Fremont, CA) at 100°C for 20 minutes. The slides were allowed to cool and were rinsed three times in PBS, pH 4.7. CytoQ Background Buster (Innovex Biosciences, Richmond, CA) was used to block for 30 minutes at room temperature in a humid chamber. All slides were then incubated with a 1:100 dilution of rabbit monoclonal anti-cytokeratin 5 (clone EP1601Y, Abcam, Cambridge, MA) and a 1:50 dilution of monoclonal mouse anti-human cytokeratin 10 (clone DE-K10, Dako, Carpinteria, CA) in primary antibody diluting buffer (Biomeda Corp, Foster City, CA) overnight at 4°C. The slides were washed three times in PBS and then incubated with 1:250 dilutions of the secondary antibodies Alexa Fluor 488 goat anti-mouse IgG and Alexa Fluor 555 goat anti-rabbit IgG (Invitrogen, Eugene, OR) for 1 hour at room temperature, in the dark. Following three final washes in PBS, the slides were mounted with ProLong Gold antifade reagent with DAPI (Invitrogen, Eugene, OR). Negative controls had one or both primary antibodies omitted, and no non-specific staining was observed (results not shown). All slides were photographed under identical conditions at 20x magnification using a fluorescent microscope.

RNA extraction and quantitative RT-PCR

Frozen wound samples and control skin were removed from −80°C storage, and the ventral epidermis was mechanically separated from the dermis using a single-edged razor blade (18). The ventral dermis was further separated from the underlying cartilage, and the cartilage and unwounded dorsal skin were discarded. Each tissue compartment (epidermis, dermis) was homogenized independently in TRIzol Reagent (Invitrogen, Eugene, OR) using 2.5 mm zirconia/silica beads in a Mini-Beadbeater bead mill (Biospec Products, Inc., Bartlesville, OK). Total RNA was extracted and purified using the RNeasy kit (Qiagen, Valencia, CA) as previously described (19). Reverse transcription was performed using one microgram of total RNA and M-MLV Reverse Transcriptase (Promega, Madison, WI) as per the manufacturer's instructions. Quantitative real-time PCR was performed on an ABI Prism 7000 Sequence Detection System (Applied Biosystems, Foster City, CA). Each PCR reaction was run in triplicate and contained 0.03μg cDNA template along with 900 nM primers and 250nM probe (see Table 1 for sequences) and Taq Man Universal Master Mix (Applied Biosystems, Foster City, CA) in a final reaction volume of 25 μL. Cycling parameters were: 50°C for 2 minutes, 95°C for 10 minutes to activate DNA polymerase, and then 40 cycles of 95°C for 15 seconds and 60°C for 1 minute. No-template controls were run in parallel to evaluate for amplification of genomic DNA. After thermal cycling, the relative mRNA expression of each amplicon was calculated by normalizing its Ct value relative to a housekeeping molecule (18s) and then expressing the value as a proportion of baseline levels (unwounded skin)($2^{-\Delta\Delta Ct}$).

Statistical analysis

All parameters were assessed using a one-sided ANOVA or using a paired t-test, with a p value of <0.05 indicating significance.

NIH-PA Author Manuscript

NIH-PA Author Manuscript

NIH-PA Author Manuscript

Results

In vitro validation of graded occlusion

In order to elucidate whether epidermal occlusion affects dermal hypertrophy (scarring), an *in vitro* method was needed to quantify the occlusive properties of the dressings to be used *in vivo*. A novel model was generated in which increasing numbers of layers of a semi-occlusive dressing (Tegaderm) were applied to a surface to achieve a graded level of occlusion. This model was validated by measuring the moisture vapor loss from a water-saturated sponge *in vitro*. The application of a single layer of the dressing resulted in a decrease in moisture loss of 30.5g/m^2/hour ($p<0.01$, Figure 1), a value equivalent to the manufacturer's specifications for the dressing. Increasing numbers of layers resulted in a logarithmic reduction in the moisture loss through the dressings. Maximal occlusion was achieved with 5 layers of semi-occlusive dressing, and this value was equivalent to silicone gel, which is used as the standard-of-care in reducing scarring in a clinical setting. In all cases, there remained some slight moisture loss through the dressing, indicating that the silicone gel (and the equivalent 5-layer dressing) is not completely occlusive, a finding which is consistent with previous studies (7).

In vivo skin hydration and trans-epidermal water loss (TEWL) measurements

Using the rabbit hypertrophic scar model (13), the effects of graded occlusion were tested *in vivo*. The three treatment groups selected were 1) no occlusion, 2) partial occlusion (1 layer of Tegaderm), and 3) maximal occlusion (5 layers of Tegaderm). Following 10 days of occlusive treatment, the dressings were removed and the skin hydration was measured using a Skicon-200 skin surface hygrometer. The Skicon-200 measures the hydration of the stratum corneum via high frequency conductance (20). The application of a single layer of semi-occlusive dressing significantly increased the hydration of the stratum corneum, and that maximal occlusion was marginally more efficacious (Figure 2A). To determine whether this increase in stratum corneum hydration was associated with an increase in overall skin hydration, the skin was allowed to equilibrate to room air for 2 hours, and the trans-epidermal water loss was measured. As with the surface hydration, partial occlusion was sufficient to significantly increase the overall skin hydration and TEWL, and maximal occlusion was marginally more efficacious (Figure 2B).

Effect of occlusion on scar formation

Under normal experimental conditions, 7mm full-thickness wounds created on the rabbit ear reliably heal with the formation of a hypertrophic scar after 28 days (13). In the current study, histological sections of control wounds were analyzed and the scar area was measured. Control wounds had a scar elevation index (SEI) of 1.62 (Figure 3), indicating that the scar dermis was 1.62 times thicker than normal dermis. Further, the control scars demonstrated marked epidermal thickening, dermal fibroplasia as well as extensive disorganization of the dermal extracellular matrix, as compared to normal skin (Figure 4).

Both methods of occlusive treatment were effective in reducing the dermal hypertrophy by 50%, as compared to the untreated controls ($p<0.05$, Figure 4). This amount of scar reduction is consistent with that observed previously using silicone gel as the therapeutic (results not shown). Within the time frame of this study, however, occlusion did not have a significant effect on the dermal collagen density, organization, or proteoglycan deposition (quantitative and qualitative analysis performed, results not shown). Further, occlusion did not affect the overall thickness of the epidermis. However, the proportion of keratinocytes demonstrating a less differentiated phenotype was found to be increased in occluded wounds. Keratin 5 is expressed by basal, undifferentiated keratinocytes, while keratin 10 is expressed by differentiating keratinocytes in the stratum spinosum and outer epidermal

NIH-PA Author Manuscript

NIH-PA Author Manuscript

NIH-PA Author Manuscript

layers (21). In histological sections co-stained with antibodies to both keratins, the ratio of keratin 5 to keratin 10 was increased in wounds treated with an occlusive dressing, and that this response was dose-dependent (Figure 5).

Quantitative RT-PCR

Total RNA was independently extracted from the epidermis and dermis of unwounded skin as well as control and occluded wounds, and mRNA expression was evaluated using quantitative reverse-transcriptase PCR. All expression was normalized to the housekeeper 18S RNA (Table 1), and unwounded skin was used as the calibrator. Specificity of the epidermal and dermal extractions was confirmed by comparing the ratio of expression of keratin 5 and vimentin (results not shown).

Epidermal samples were evaluated for the production of mRNA for keratin 5 and keratin 10 (Figure 6). As observed by immunohistochemistry, the expression of both keratins was increased in control scars as compared to unwounded skin. This indicates an increased metabolic activity in the scars. Notably, keratin 5 expression was further upregulated in occluded wounds, which corroborates the immunohistochemistry results.

The epidermal samples were also evaluated for the production of mRNA for the pro-inflammatory cytokines interleukin-1 beta (IL-1β) and tumor necrosis factor alpha (TNF-α) (Figure 7). Both cytokines were significantly upregulated in control scars as compared to unwounded skin. Occlusion significantly decreased the expression of IL-1β in a dose-dependent fashion, and maximal occlusion by the application of 5 layers of Tegaderm significantly increased the expression of TNF-α as compared to control wounds.

Dermal samples were evaluated for the expression of members of the pro-fibrotic transforming growth factor-beta (TGF-β) family, and related signaling molecules (Figure 8). Significant alterations in the TGF-β signaling pathway were observed. Control scars demonstrated a significant increase in the expression of both TGF-β1 and TGF-β3, as compared to unwounded skin. While occlusion had no significant effect on the expression of TGF-β1, occlusion caused a dose-dependent increase in the expression of the anti-fibrotic growth factor TGF-β3. Additionally, the expression of several TGF-β signaling molecules, including SMAD3 and SMAD7, were increased in a dose-dependent manner in response to occlusion. These findings therefore indicate that treatment of immature scars with an occlusive dressing results in changes in the epidermal expression of pro- and-anti fibrotic cytokines, and that these changes were associated with a concomitant reduction in pro-fibrotic signaling in the dermis.

Discussion

In this study, we have utilized an accepted, established animal model of wound fibrosis (New Zealand White rabbit ear hypertrophic scar model) to confirm that various levels of occlusion are effective at reducing scar formation *in vivo*. We have confirmed that the degree of occlusion affects the hydration state of the epidermis, and that this affects the degree of epidermal differentiation, as indicated by keratin expression (keratin 5 and 10). We also investigated the molecular expression pattern of the occluded and non-occluded epidermis and dermis, and have confirmed that several of the factors that are altered upon keratinocyte hydration *in vitro* (IL-1β, TNF-α) are also affected *in vivo.* Furthermore, this results in concomitant changes in the expression of pro-fibrotic signaling molecules (TGF-β, SMADs) within the dermis. Taken together, this data strongly supports the hypothesis that the mechanism of action of silicone gel and other occlusive therapies is by increasing the hydration of the epidermis and by reducing the production of pro-fibrotic signals by activated keratinocytes.

NIH-PA Author Manuscript

NIH-PA Author Manuscript

NIH-PA Author Manuscript

This investigation has confirmed that epidermal occlusion *in vivo* results in an increase in epidermal hydration and in decreased keratinocyte activation, as demonstrated by an increased expression of the "basal" keratins (keratin 5) relative to the "differentiated" and "activated" keratins (keratin 10, 16 and others)(21). This may be important to the regulation of fibrosis and scarring, as a link has been identified between keratinocyte activation, keratin expression, and inflammation. In keratin 5 $^{-/-}$ mice and in a cell culture model of epidermolysis bullosa simplex (HaCaT keratinocytes with a mutation in keratin 14, another basal keratin), production of the pro-inflammatory cytokines IL-1β and IL-6 is increased (22). Therefore, it is possible that the increased expression of the basal keratins in occluded wounds allows for a down-regulation of pro-inflammatory and pro-fibrotic factors in the skin following wounding. Other recent studies have shown that epidermal thickness may decrease following treatment with various methods of occlusion (6, 7, Jia SX and Mustoe TA, unpublished observations). In those studies, keratinocyte activation is also reduced following occlusive treatment. Therefore, further investigations are required to further elucidate the role of activated keratinocytes in scar formation.

Interleukin 1 (IL-1) is a pro-inflammatory cytokine that is involved in the initiation of wound repair. Its two isoforms, IL-1α and IL-1β, are sequestered in pre-formed intracellular pools within quiescent keratinocytes (23,24) and can be released or synthesized *de novo* by activated keratinocytes (11,25). Both isoforms signal through the IL-1 type I receptor (26), which stimulates the autocrine production of IL-1, IL-8, and other factors (21) (review). *In vivo* studies performed in our laboratory have demonstrated that keratinocyte-produced IL-1 (and other cytokines) also diffuses through a mature, stratified epithelium, and affect fibroblasts in a paracrine manner (11). IL-1 has been shown to affect fibroblast proliferation and migration, as well as affecting the production of growth factors and extracellular matrix components by fibroblasts (26,27). Of interest, the level of IL-1 expression has been shown to directly correlate with the degree of fibrosis in other tissues as well, and bleomycin-induced lung fibrosis may be reduced by blocking IL-1 via the production and release of IL-1 receptor antagonist by mesenchymal stem cells (28). Additionally, there may be cross-talk between IL-1β and transforming growth factor beta (TGF-β), whereby each may bind to and activate the opposite receptors (IL-1R and TBRI and II, respectively) when the ligand is present at very high concentrations (29). This reciprocal relationship may be another way in which epidermal-secreted IL-1 may stimulate the production of extracellular matrix molecules by dermal fibroblasts following a cutaneous injury. In this study, the level of epidermal IL-1β mRNA expression directly correlates with the amount of dermal fibrosis in our rabbit ear model. Untreated wounds, which form a hypertrophic scar, demonstrated a high level of IL-1β expression in the dermis well after re-epithelialization was complete. In contrast, occluded wounds, which form a significantly smaller scar, had a significantly lower expression of IL-1β. This suggests that IL-1 may be a major factor that enables epidermal keratinocytes to affect fibroblast activation and regulate fibrosis and scarring. We are in the process of investigating the effect of IL-1 on dermal fibrosis; recent studies in our laboratory indicate that increased IL-1β production by injured keratinocytes modulates dermal fibroblast behavior and collagen synthesis *in vivo* in the absence of a dermal injury (Gallant-Behm *et al*, manuscript in preparation). Furthermore, those studies have determined that an IL-1 antagonist is effective at altering fibroblast gene expression and in reducing scar formation in the absence of occlusive therapy (Gallant-Behm *et al*, manuscript in preparation). Additional recent studies (30) have suggested that IL-1 inhibition may also result in a better tissue architecture following wound repair.

The current study also revealed that tumor necrosis factor-alpha (TNF-α) expression was increased in the epidermis of occluded wounds. TNF-α is highly pro-inflammatory, and is upregulated in many chronic conditions including rheumatoid arthritis and inflammatory bowel disease (31)(review). However, there is a growing body of evidence that suggests that

NIH-PA Author Manuscript

NIH-PA Author Manuscript

NIH-PA Author Manuscript

TNF-α may have anti-fibrotic functions. Not only has TNF-α been shown to directly inhibit alpha-2 (I) collagen (COL1A2) gene transcription (32,33), but TNF-α also suppress the TGF-β-induced expression of CTGF protein in cultured normal fibroblasts (34). Furthermore, TNF-α also stimulates the expression of the matrix metalloproteinases (35), thereby contributing to collagen degradation. Taken together, this indicates that TNF-α may act on multiple levels to reduce collagen synthesis and fibrosis by fibroblasts, and that IL-1 and TNF-α may act in concert to affect fibroblast behavior *in vitro* and *in vivo*. This may help to explain how the cutaneous epidermis regulates dermal fibrosis following injury. This hypothesis is supported by the observation that primary epidermal keratinocytes inhibit fibroblast collagen synthesis *in vitro* by the secretion of soluble mediators, including TNF-α, which is upregulated by hydration (11).

One major limitation of the current study is that the *in vitro* measurement of water vapor loss does not completely correlate with the *in vivo* results. Specifically, five layers of Tegaderm resulted in a significant drop in water vapor loss *in vitro* as compared to one layer of Tegaderm (Figure 1), but the two treatments were not significantly different in terms of epidermal hydration and TEWL (Figure 2) or in their effect on dermal scarring (Figure 3). However, it is important to note that in our animal model, by the time the occlusive treatment was applied the epidermis did have an immature stratum corneum that also provided some water-retention capabilities. Therefore, multiple layers of Tegaderm applied to the skin may not have increased the water content of the epidermis (as compared to a single layer of Tegaderm) beyond the measurement capabilities of the devices and tests used. It is important to note that the histologic and molecular analysis did identify some differences between the two treatments, indicating that increasing levels of occlusion do in fact affect the epidermal behavior. Furthermore, previous studies in this laboratory (7) have demonstrated that complete occlusion does cause a significant decrease in hypertrophic scarring, as compared to silicone gel (equivalent to 5 layers of Tegaderm in this study).

Another limitation of the current study is that we have only identified two mechanisms by which keratinocytes may influence fibroblast activation and extracellular matrix production (IL-1β and TNF-α). It is quite likely that there are other factors that also play a role in this process. For instance, it has been suggested that keratinocyte-derived 14-3-3σ (stratifin) may stimulate matrix metalloproteinase expression and decrease collagen expression in fibroblasts (36). We are currently in the process of performing a microarray analysis on epidermal samples to determine whether there are other novel factors produced by keratinocytes that may regulate fibroblast function and scar formation.

Transforming growth factor-beta (TGF-β) is a pleiotropic growth factor that is produced by numerous cell types including inflammatory cells, endothelial cells, keratinocytes, and fibroblasts, and TGF-β plays a major role in the regulation of the wound healing process (37) review. TGF-β has been shown to stimulate fibroblast chemotaxis, proliferation, differentiation, cytokine production, extracellular matrix synthesis, and contraction (37) through TGF-β receptor I and II. The resulting signaling cascade occurs via the phosphorylation of SMAD 2, 3, and 4, whereas SMAD7 is an endogenous antagonist (37). The primary TGF isoform, TGF-β1, is believed to be pro-fibrotic, and the expression of TGF-β1 has been shown to be increased in hypertrophic scars (38). Another isoform, TGF-β3, is believed to be anti-fibrotic, and TGF-β3 treatment has been shown to reduce cutaneous scarring in an animal model (39). Therefore, skin fibrosis may be regulated not only by the absolute level of TGF-β expression, but also by the ratio of TGF-β1 to TGF-β3, and by the relative abundance of SMAD2/3/4 and SMAD7. In this study, the expression of TGF-β1 and 3, of SMAD3 and 7 was measured in occluded and non-occluded rabbit ear wounds. A highly significant observation was that the expression of TGF-β1 was unaffected by occlusion, but that TGF-β3 was increased, thereby reducing the overall ratio of TGF-β1

NIH-PA Author Manuscript

NIH-PA Author Manuscript

NIH-PA Author Manuscript

to TGF-β3 more than 2-fold. Similarly, while SMAD3 was upregulated following occlusion, SMAD7 had a greater upregulation, resulting in an overall increase in the amount of antagonist. Thus, the observed decrease in scar fibrosis following occlusive therapy was likely affected by this altered TGF-β signaling in the scar dermis. Further work is needed to determine if the changes in epidermal cytokine expression are acting via the TGF-β signaling pathway, or if other pathways may be involved.

In summary, this study has confirmed that the application of an occlusive therapeutic to a newly healed wound is indeed beneficial in preventing the formation of a hypertrophic scar. The mode of action of this therapy is by the hydration of epidermal keratinocytes, which in turn results in a decrease in the expression of pro-inflammatory cytokines (IL-1) and an increase in the expression of anti-fibrotic cytokines (TNF-α) by the wound keratinocytes. These signaling changes are correlated with alterations in the activation state of the dermal fibroblasts, resulting in less extracellular matrix synthesis and less scarring. While occlusive therapy alone remains moderately effective at reducing scar formation, it may be possible to develop alternative therapeutics based on this research that will more selectively target the keratinocyte signaling molecules and enhance scar prevention and treatment strategies.

Acknowledgments

Funding provided in part by NIH P20 GM078426-01

Abbreviations

IL-1β	Interleukin-1 beta
POD	Post-operative day
SEI	Scar elevation index
TEWL	Trans-epidermal water loss
TGF-β	Transforming growth factor beta
TNF-α	Tumor necrosis factor alpha

References

1. O'Brien L, Pandit A. Silicon gel sheeting for preventing and treating hypertrophic and keloid scars. Cochrane Database Syst Rev. 2006; (1):CD003826. [PubMed: 16437463]
2. Mustoe TA, Cooter RD, Gold MH, Hobbs FD, Ramelet AA, Shakespeare PG, Stella M, Teot L, Wood FM, Ziegler UE. International clinical recommendations on scar management. Plast Reconstr Surg. 2002; 110(2):560–71. [PubMed: 12142678]
3. Ahn ST, Monafo WW, Mustoe TA. Topical silicone gel: a new treatment for hypertrophic scars. Surgery. 1989; 106(4):781–6. discussion 786–7. [PubMed: 2529659]
4. Mustoe TA. Evolution of silicone therapy and mechanism of action in scar management. Aesthetic Plast Surg. 2008; 32(1):82–92. [PubMed: 17968615]
5. Saulis AS, Chao JD, Telser A, Mogford JE, Mustoe TA. Silicone occlusive treatment of hypertrophic scar in the rabbit model. Aesthet Surg J. 2002; 22(2):147–53. [PubMed: 19331964]
6. O'Shaughnessy KD, De La Garza M, Roy NK, Mustoe TA. Homeostasis of the epidermal barrier layer: a theory of how occlusion reduces hypertrophic scarring. Wound Repair Regen. 2009; 17(5): 700–8. [PubMed: 19769722]
7. Tandara AA, Mustoe TA. The role of the epidermis in the control of scarring: evidence for mechanism of action for silicone gel. J Plast Reconstr Aesthet Surg. 2008; 61(10):1219–25. [PubMed: 18653391]

NIH-PA Author Manuscript

NIH-PA Author Manuscript

NIH-PA Author Manuscript

8. Kloeters O, Schierle C, Tandara A, Mustoe TA. The use of a semiocclusive dressing reduces epidermal inflammatory cytokine expression and mitigates dermal proliferation and inflammation in a rat incisional model. Wound Repair Regen. 2008; 16(4):568–75. [PubMed: 18638276]
9. Sawada Y, Sone K. Hydration and occlusion treatment for hypertrophic scars and keloids. Br J Plast Surg. 1992; 45(8):599–603. [PubMed: 1493533]
10. Sawada Y, Sone K. Treatment of scars and keloids with a cream containing silicone oil. Br J Plast Surg. 1990; 43(6):683–8. [PubMed: 2104531]
11. Tandara AA, Kloeters O, Mogford JE, Mustoe TA. Hydrated keratinocytes reduce collagen synthesis by fibroblasts via paracrine mechanisms. Wound Repair Regen. 2007; 15(4):497–504. [PubMed: 17650093]
12. Chang CC, Kuo YF, Chiu HC, Lee JL, Wong TW, Jee SH. Hydration, not silicone, modulates the effects of keratinocytes on fibroblasts. J Surg Res. 1995; 59(6):705–11. [PubMed: 8538169]
13. Kloeters O, Tandara A, Mustoe TA. Hypertrophic scar model in the rabbit ear: a reproducible model for studying scar tissue behavior with new observations on silicone gel sheeting for scar reduction. Wound Repair Regen. 2007; 15 (Suppl 1):S40–5. [PubMed: 17727466]
14. Harada T, Izaki S, Tsutsumi H, Kobayashi M, Kitamura K. Apoptosis of hair follicle cells in the second-degree burn wound unders hypernatremic conditions. Burns. 1998; 24(5):464–9. [PubMed: 9725689]
15. Junqueira LC, Bignolas G, Brentani RR. Picrosirius staining plus polarization microscopy, a specific method for collagen detection in tissue sections. Histochem J. 1979; 11(4):447–55. [PubMed: 91593]
16. Camplejohn KL, Allard SA. Limitations of safranin 'O' staining in proteoglycan-depleted cartilage demonstrated with monoclonal antibodies. Histochemistry. 1988; 89(2):185–8. [PubMed: 3135283]
17. Cook, HC. Carbohydrates: Theory and practice of histological techniques. 3. Bancroft, J.; Stevens, A., editors. Edinburgh: Churchill Livingstone; 1990.
18. Schierle C, O'Shaughnessy K, Ding XZ, Galiano RD, Mustoe TA. Silicone gel occlusion suppresses epidermal activation in a murine cutaneous wound model. Wound Repair Regen. 2007; 15(2):A23.
19. Reno C, Marchuk L, Sciore P, Frank CB, Hart DA. Rapid isolation of total RNA from small samples of hypocellular, dense connective tissues. Biotechniques. 1997; 22(6):1082–6. [PubMed: 9187757]
20. Hashimoto-Kumasaka K, Takahashi K, Tagami H. Electrical measurement of the water content of the stratum corneum in vivo and in vitro under various conditions: comparison between skin surface hygrometer and corneometer in evaluation of the skin surface hydration state. Acta Derm Venereol. 1993; 73(5):335–9. [PubMed: 7904396]
21. Freedberg IM, Tomic-Canic M, Komine M, Blumenberg M. Keratins and the keratinocyte activation cycle. J Invest Dermatol. 2001; 116(5):633–40. [PubMed: 11348449]
22. Lu H, Chen J, Planko L, Zigrino P, Klein-Hitpass L, Magin TM. Induction of inflammatory cytokines by a keratin mutation and their repression by a small molecule in a mouse model for EBS. J Invest Dermatol. 2007; 127(12):2781–9. [PubMed: 17581617]
23. Hauser C, Saurat JH, Schmitt A, Jaunin F, Dayer JM. Interleukin 1 is present in normal human epidermis. J Immunol. 1986; 136(9):3317–23. [PubMed: 3007615]
24. Kupper TS, Ballard DW, Chua AO, McGuire JS, Flood PM, Horowitz MCR, Langdon R, Lightfoot L, Gubler U. Human keratinocytes contain mRNA indistinguishable from monocyte interleukin 1 alpha and beta mRNA. Keratinocyte epidermal cell-derived thymocyte-activating factor is identical to interleukin 1. J Exp Med. 1986; 164(6):2095–100. [PubMed: 2431094]
25. Blanton RA, Kupper TS, McDougall JK, Dower S. Regulation of interleukin 1 and its receptor in human keratinocytes. Proc Natl Acad Sci U S A. 1989; 86(4):1273–7. [PubMed: 2465548]
26. Yano S, Banno T, Walsh R, Blumenberg M. Transcriptional responses of human epidermal keratinocytes to cytokine interleukin-1. J Cell Physiol. 2008; 214(1):1–13. [PubMed: 17941080]
27. Maas-Szabowski N, Fusenig NE. Interleukin-1-induced growth factor expression in postmitotic and resting fibroblasts. J Invest Dermatol. 1996; 107(6):849–55. [PubMed: 8941673]

NIH-PA Author Manuscript

NIH-PA Author Manuscript

NIH-PA Author Manuscript

28. Ortiz LA, Dutreil M, Fattman C, Pandey AC, Torres G, Go K, Phinney DG. Interleukin 1 receptor antagonist mediates the antiinflammatory and antifibrotic effect of mesenchymal stem cells during lung injury. Proc Natl Acad Sci U S A. 2007; 104(26):11002–7. [PubMed: 17569781]
29. Lu T, Tian L, Han Y, Vogelbaum M, Stark GR. Dose-dependent cross-talk between the transforming growth factor-beta and interleukin-1 signaling pathways. Proc Natl Acad Sci U S A. 2007; 104(11):4365–70. [PubMed: 17360530]
30. Thomay AA, Daley JM, Sabo E, Worth PJ, Shelton LJ, Harty MW, Reichner JS, Albina PE. Disruption of interleukin-1 signaling improves the quality of wound healing. Am J Pathol. 2009; 174(6):2129–36. [PubMed: 19389930]
31. Sethi G, Sung B, Aggarwal BB. TNF: a master switch for inflammation to cancer. Front Biosci. 2008; 13:5094–107. [PubMed: 18508572]
32. Kouba DJ, Chung KY, Nishiyama T, Vindevoghel L, Kon A, Klement JF, Uitto J, Mauviel A. Nuclear factor-kappa B mediates TNF-alpha inhibitory effect on alpha 2(I) collagen (COL1A2) gene transcription in human dermal fibroblasts. J Immunol. 1999; 162(7):4226–34. [PubMed: 10201951]
33. Greenwel P, Tanaka S, Penkov SD, Zhang W, Olive M, Moll J, Vinson C, Di Liberto M, Ramirez F. Tumor necrosis factor alpha inhibits type I collagen synthesis through repressive CCAAT/enhancer-binding proteins. Mol Cell Biol. 2000; 20(3):912–8. [PubMed: 10629048]
34. Abraham DJ, Shiwen X, Black CM, Sa S, Xu Y, Leask A. Tumor necrosis factor alpha suppresses the induction of connective tissue growth factor by transforming growth factor-beta in normal and scleroderma fibroblasts. J Biol Chem. 2000; 275(20):15220–5. [PubMed: 10809757]
35. Dollery CM, McEwan JR, Henney AM. Matrix metalloproteinases and cardiovascular disease. Circ Res. 1995; 77(5):863–8. [PubMed: 7554139]
36. Ghaffari A, Li Y, Karami A, Ghaffari M, Tredget EE, Ghahary A. Fibroblast extracellular matrix gene expression in response to keratinocyte-releasable stratifin. J Cell Biochem. 2006; 98(2):383–93. [PubMed: 16440305]
37. Varga J. Scleroderma and Smads: dysfunctional Smad family dynamics culminating in fibrosis. Arthritis Rheum. 2002; 46(7):1703–13. [PubMed: 12124852]
38. Kryger ZB, Sisco M, Roy NK, Lu L, Rosenberg D, Mustoe TA. Temporal expression of the transforming growth factor-Beta pathway in the rabbit ear model of wound healing and scarring. J Am Coll Surg. 2007; 205(1):78–88. [PubMed: 17617336]
39. Shah M, Foreman DM, Ferguson MW. Neutralisation of TGF-beta 1 and TGF-beta 2 or exogenous addition of TGF-beta 3 to cutaneous rat wounds reduces scarring. J Cell Sci. 1995; 108 (Pt 3):985–1002. [PubMed: 7542672]

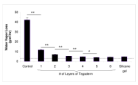

Figure 1.

In vitro validation of occlusive dressing treatments. The water vapor loss from a water saturated sponge was measured under standardized environmental conditions (21°C, 35% humidity). The application of a semi-occlusive film dressing (Tegaderm) resulted in a decrease in 30.5g/m^2/hour, a value equivalent to the manufacturer's specifications for the dressing. Maximal occlusion was achieved with 5 layers of semi-occlusive dressing, or with the application of a silicone gel. Dashed line = baseline. ** $p<0.01$, * $p<0.05$, N=5.

NIH-PA Author Manuscript
NIH-PA Author Manuscript
NIH-PA Author Manuscript

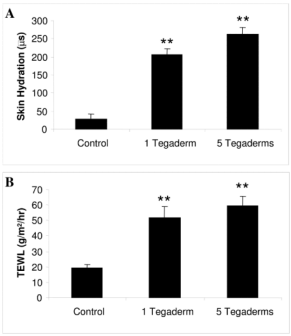

Figure 2.

In vivo skin hydration and TEWL measurement. On post-operative day 28, the occlusive dressings were removed and the scars were allowed to acclimate to room air for two hours. The skin hydration (A) and trans-epidermal water loss (B) were measured. Occlusive treatment significantly increased the hydration of the scar, which in turn increased the TEWL measurement. N=9 per treatment. ** $p<0.01$.

NIH-PA Author Manuscript
NIH-PA Author Manuscript
NIH-PA Author Manuscript

NIH-PA Author Manuscript

NIH-PA Author Manuscript

NIH-PA Author Manuscript

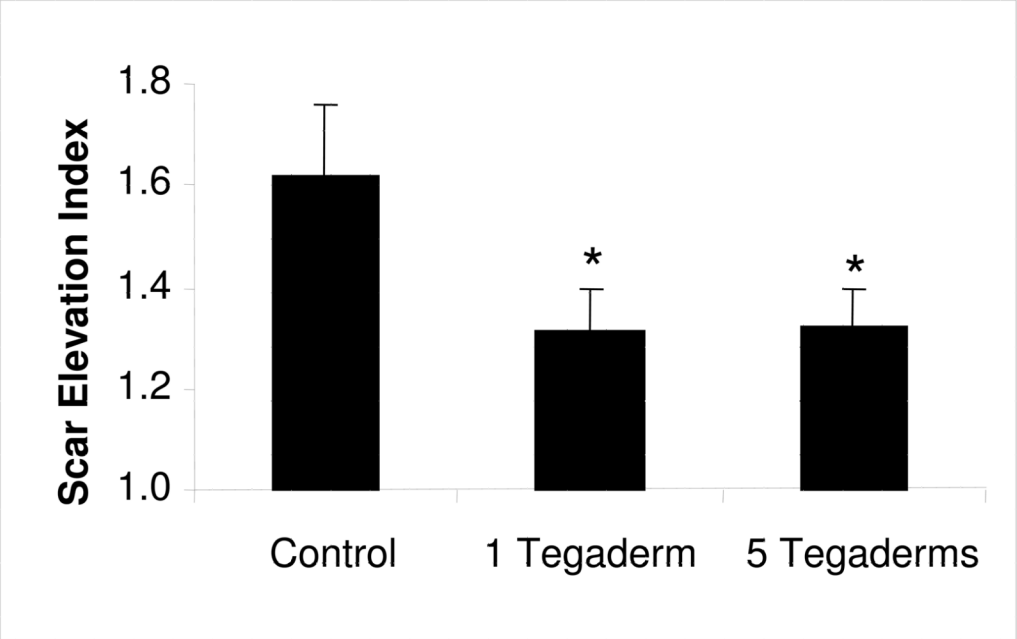

Figure 3.
Quantification of scar volume. The scar elevation index (SEI) was measured using hematoxylin and eosin stained histology sections of wounds harvested at postoperative day 28. An SEI of 1 indicates the scar is of equal height to the surrounding unwounded skin; an SEI greater than 1 represents a raised, hypertrophic scar. All methods of occlusion significantly reduced the amount of hypertrophic scarring to a level equivalent to that of wounds treated with silicone gel. N=9 per treatment. * $p<0.05$.

NIH-PA Author Manuscript
NIH-PA Author Manuscript
NIH-PA Author Manuscript

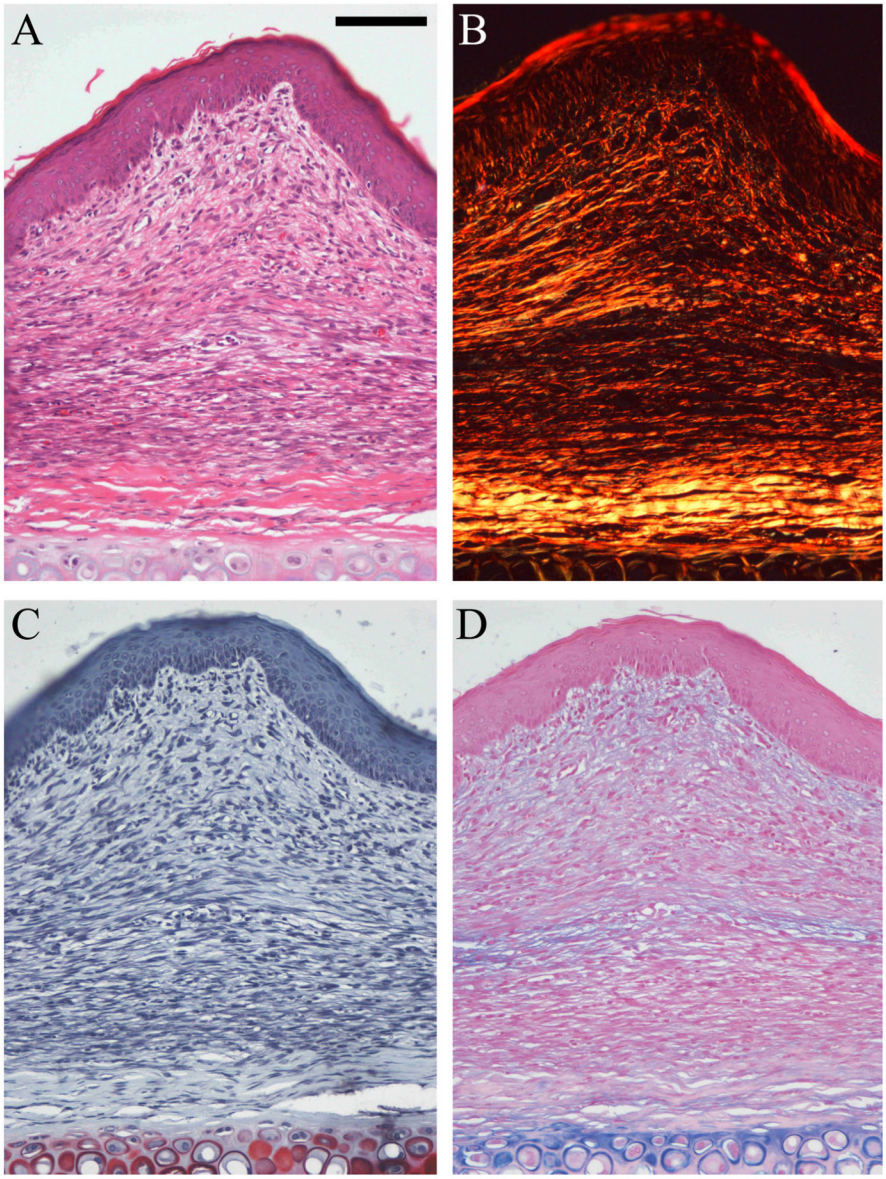

Figure 4.
Histology staining. Representative photomicrographs of control scars stained with hematoxylin and eosin (A), sirius red (B), safranin O/fast green (C), and alcian blue (D). Magnification 20X. Scale bar = 100μm. The scars (POD28) demonstrate a thickened epidermis, dermal fibroplasia and dermal hypertrophy (A) as compared to unwounded skin. The extracellular matrix consists of fine, disorganized collagen fibers (B), and small amounts of proteoglycans, diffusely deposited in the dermis (C and D). Occluded scars do not significantly differ from control scars except for their reduced hypertrophy.

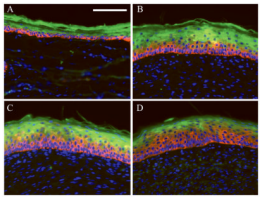

Figure 5.
Cytokeratin immunohistochemistry. Red = Keratin 5. Green = Keratin 10. Blue = DAPI. (A) Normal, unwounded skin, (B) control scar, (C) 1 Tegaderm, (D) 5 Tegaderms. Magnification 20X. Scale bar = 100mm. Occlusion increased the proportion of keratinocytes expressing keratin 5 (basal keratinocytes) as compared to keratin 10 (differentiated keratinocytes).

NIH-PA Author Manuscript
NIH-PA Author Manuscript
NIH-PA Author Manuscript

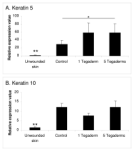

Figure 6.

Epidermal mRNA expression of keratin 5 (A), keratin 10 (B). Expression of keratin 5 and 10 is elevated in hypertrophic scars, and expression of keratin 5 is further increased by occlusion. N=9 per treatment. * $p<0.05$, ** $p<0.01$.

NIH-PA Author Manuscript
NIH-PA Author Manuscript
NIH-PA Author Manuscript

NIH-PA Author Manuscript

NIH-PA Author Manuscript

NIH-PA Author Manuscript

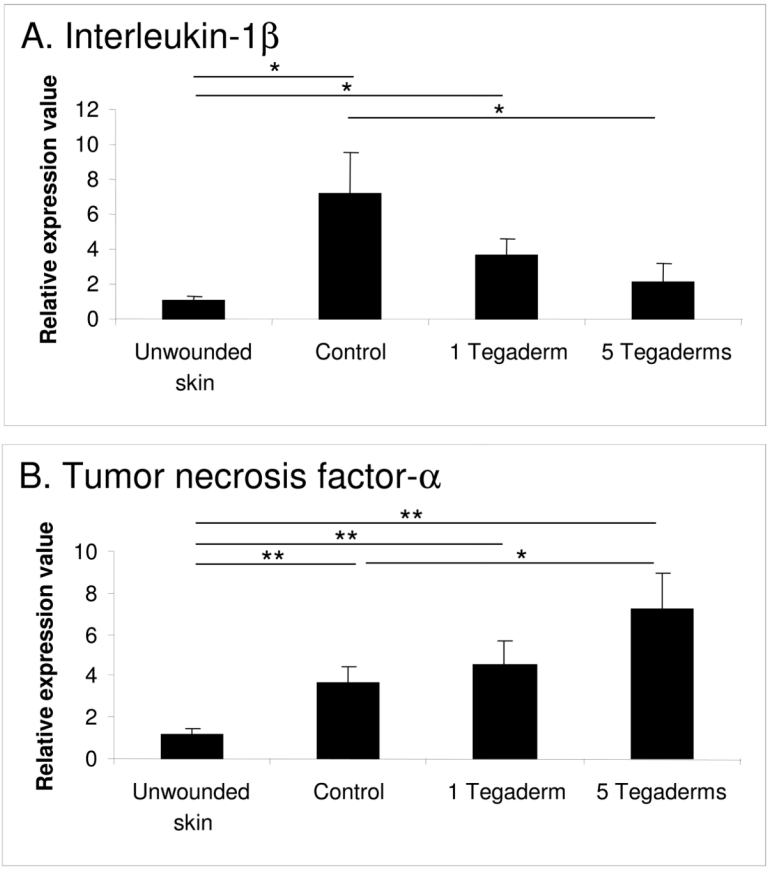

Figure 7.

Epidermal mRNA expression of interleukin-1β (IL-1β) (A) and tumor necrosis factor-α (TNF-α) (B). Expression of IL-1β is elevated in hypertrophic scars, and this elevation is suppressed by occlusion. Expression of TNF-α is increased by occlusion. N=9 per treatment. * $p<0.05$.

NIH-PA Author Manuscript

NIH-PA Author Manuscript

NIH-PA Author Manuscript

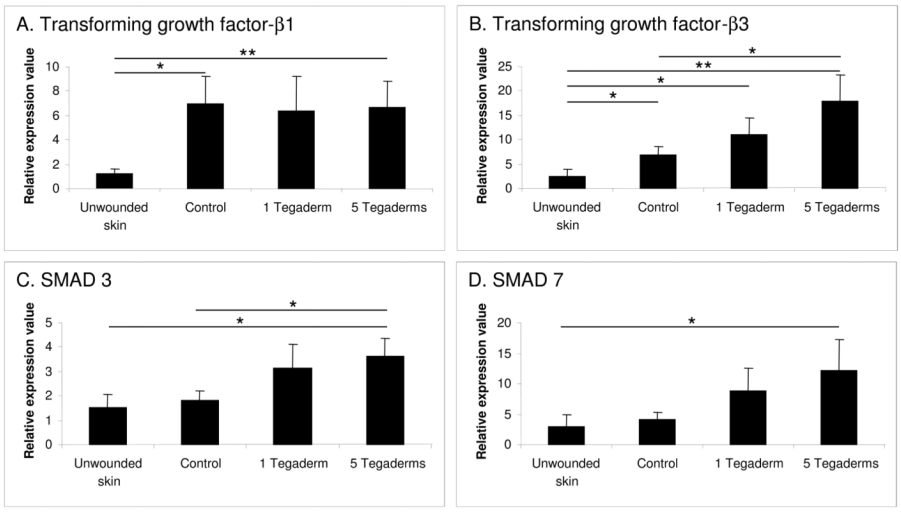

Figure 8.

Dermal mRNA expression of transforming growth factor-β1 (TGF-β1) (A), TGF-β3 (B), SMAD3 (C), and SMAD7 (D). Expression of TGF-β1 and TGF-β3 is elevated in hypertrophic scars, and expression of TGF-β3, SMAD3, and SMAD4 is increased by occlusion in a dose-responsive fashion. N=9 per treatment. * $p<0.05$, ** $p<0.01$.

NIH-PA Author Manuscript

NIH-PA Author Manuscript

NIH-PA Author Manuscript

Table 1

Oligonucleotide primer and probe sequences used for real-time PCR.

Gene	Sequence
18S	Forward: 5′-GCCGCTAGAGGTGAAATTCTTG-3′ Reverse: 5′-CATTCTTGGCAAATGCTTTCG-3′ Probe: 5′-ACCGGCGCAAGACGGACCAG-3′
IL-1β	Forward: 5′-CAGGCTCCAGGATGCACAA-3′ Reverse: 5′-AGGTGGAGAGCTTTCAGCTCAT-3′ Probe: 5′-AGAAATCCCTGGTGTTGTCTGGCACG-3′
Keratin 5	Forward: 5′-TGCCTCCTTCATTGACAAGGT-3′ Reverse: 5′-CAGCAGCTCCCATTTCGTTT-3′ Probe: 5′-CGGTTCCTGGAGCAGCAGAACCA-3′
Keratin 10	Forward: 5′-CAGGATGAAGTATGAGAACGAGGTT-3′ Reverse: 5′-TGCGCAGCCCGTTGAT-3′ Probe: 5′-CCCTGCGCCAGAGCGTGGAG-3′
TGF-β1	Forward: 5′-TGCGGCAGCTGTACATTGAC-3′ Reverse: 5′-GGCAGAAGTTGGCGTGGTA-3′ Probe: 5′-AAGGACCTGGGCTGGAAGTGGATCC-3′
TGF-β3	Forward: 5′-CGGCTCAAGAAGCAGAAGGA-3′ Reverse: 5′-CGGTGCGGTGGAATCATC-3′ Probe: 5′-CACCACAACCCTCACCTCATCCTC-3′
TNF-α	Forward: 5′-TGGTCACCCTCAGATCAGCTT-3′ Reverse: 5′-CTTGCGGGTTTGCTACTACGT-3′ Probe: 5′-TCGGGCCCTGAGTGACGAGCC-3′
SMAD 3	Forward: 5′-CATCGAGCCCCAGAGCAATA-3′ Reverse: 5′-GTCTCTCCATCTTCGCTCAGGTA-3′ Probe: 5′-TGGCTTCTGTCCTGTGGACATTGGAG-3′
SMAD 7	Forward: 5′-GATTTTCTCAAACCAACTGCAGATT-3′ Reverse: 5′-TAATTCGTTCCCCCTGTTTCA-3′ Probe: 5′-TCCAGATGCTGTGCCTTCCTCCG-3′
Vimentin	Forward: 5′-ACAACCTGGCCGAAGACATC-3′ Reverse: 5′-GCTTCCTCTCTCTGCAGCATCT-3′ Probe: 5′-TGCGGCTCCGGGAGAAGTTGC-3′